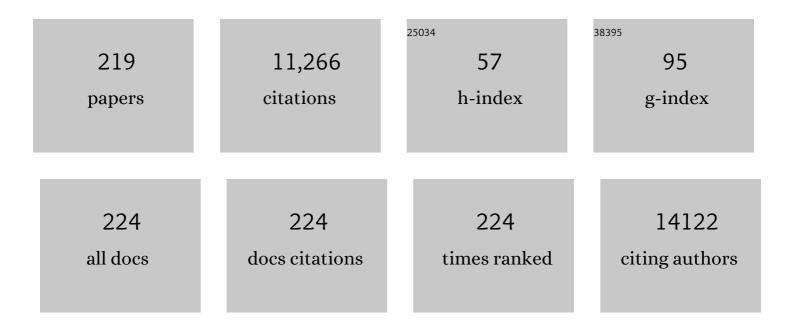
Sreekumar Kurungot

List of Publications by Year in descending order

Source: https://exaly.com/author-pdf/213568/publications.pdf Version: 2024-02-01



#	Article	IF	CITATIONS
1	The role and the necessary features of electrolytes for microsupercapacitors. , 2022, , 47-116.		3
2	Tuning of Oxygen Reduction Pathways through Structural Variation in Transition Metalâ€Đoped Ba 2 In 2 O 5. ChemElectroChem, 2022, 9, .	3.4	2
3	A pseudo-boehmite AlOOH supported NGr composite-based air electrode for mechanically rechargeable Zn-air battery applications. Journal of Materials Chemistry A, 2022, 10, 10014-10025.	10.3	11
4	Co–Ni Layered Double Hydroxide for the Electrocatalytic Oxidation of Organic Molecules: An Approach to Lowering the Overall Cell Voltage for the Water Splitting Process. ACS Applied Materials & Interfaces, 2022, 14, 16222-16232.	8.0	21
5	Enhanced proton conductivity in amino acid based self-assembled non-porous hydrogen-bonded organic frameworks. Chemical Communications, 2022, , .	4.1	2
6	Synthesis of a Highly Electron-Deficient, Water-Stable, Large Ionic Box: Multielectron Accumulation and Proton Conductivity. Organic Letters, 2022, 24, 3038-3042.	4.6	5
7	Singleâ€Step Synthesis of Exfoliated Ti ₃ C ₂ T _x MXene through NaBF ₄ /HCl Etching as Electrode Material for Asymmetric Supercapacitor. ChemistrySelect, 2022, 7, .	1.5	6
8	Electrodeposited Layered Sodium Vanadyl Phosphate (Na _{<i>x</i>} VOPO ₄ · <i>n</i> H ₂ O) as Cathode Material for Aqueous Rechargeable Zinc Metal Batteries. Energy & Fuels, 2022, 36, 6520-6531.	5.1	3
9	Air–Cathode Interface-Engineered Electrocatalyst for Solid-State Rechargeable Zinc–Air Batteries. ACS Applied Energy Materials, 2022, 5, 8756-8768.	5.1	3
10	Synergistic effect of B site co-doping with Co and Ce in bifunctional oxygen electrocatalysis by oxygen deficient brownmillerite Ba2In2O5. Catalysis Today, 2021, 375, 494-500.	4.4	8
11	Interconnected polyaniline nanostructures: Enhanced interface for better supercapacitance retention. Polymer, 2021, 212, 123169.	3.8	12
12	In Situ Preparation of Ionomer as a Tool for Tripleâ€Phase Boundary Enhancement in 3D Graphene Supported Pt Catalyst. Advanced Sustainable Systems, 2021, 5, .	5.3	6
13	Biomass-derived activated carbon material from native European deciduous trees as an inexpensive and sustainable energy material for supercapacitor application. Journal of Energy Storage, 2021, 34, 102178.	8.1	105
14	Facile synthesis of CNT interconnected PVP-ZIF-8 derived hierarchically porous Zn/N co-doped carbon frameworks for oxygen reduction. Nanoscale, 2021, 13, 6248-6258.	5.6	21
15	Naphthalene dianhydride organic anode for a â€~rocking-chair' zinc–proton hybrid ionÂbattery. Dalton Transactions, 2021, 50, 4237-4243.	3.3	12
16	<i>In situ</i> polymerization process: an essential design tool for lithium polymer batteries. Energy and Environmental Science, 2021, 14, 2708-2788.	30.8	140
17	PdP/WO ₃ multi-functional catalyst with high activity and stability for direct liquid fuel cells (DLFCs). Sustainable Energy and Fuels, 2021, 5, 4758-4770.	4.9	5
18	A high-voltage non-aqueous hybrid supercapacitor based on the N2200 polymer supported over multiwalled carbon nanotubes. Nanoscale, 2021, 13, 12314-12326.	5.6	10

#	Article	IF	CITATIONS
19	Zinc–Air Batteries Catalyzed Using Co ₃ O ₄ Nanorod-Supported N-Doped Entangled Graphene for Oxygen Reduction Reaction. ACS Applied Energy Materials, 2021, 4, 4570-4580.	5.1	14
20	Enhanced electrocatalytic activity of PtRu/nitrogen and sulphur co-doped crumbled graphene in acid and alkaline media. Journal of Colloid and Interface Science, 2021, 590, 154-163.	9.4	13
21	Seed-Mediated Growth of Pt on High-Index Faceted Au Nanocrystals: The Ag Lining and Implications for Electrocatalysis. ACS Applied Nano Materials, 2021, 4, 9155-9166.	5.0	3
22	Efficient Electrochemical Oxygen Reduction to Hydrogen Peroxide by Transition Metal-Doped Silicate Sr0.7Na0.3SiO3â^δ. ACS Applied Materials & Interfaces, 2021, 13, 382-390.	8.0	5
23	Toward pH Independent Oxygen Reduction Reaction by Polydopamine Derived 3D Interconnected, Iron Carbide Embedded Graphitic Carbon. ACS Applied Materials & Interfaces, 2021, 13, 8147-8158.	8.0	15
24	A sulfonated polyvinyl alcohol ionomer membrane favoring smooth electrodeposition of zinc for aqueous rechargeable zinc metal batteries. Sustainable Energy and Fuels, 2021, 5, 5557-5564.	4.9	3
25	Synergistic electronic coupling/cross-talk between the isolated metal halide units of zero dimensional heterometallic (Sb, Mn) halide hybrid with enhanced emission. Journal of Materials Chemistry C, 2021, 10, 360-370.	5.5	8
26	Dioxolanone-Anchored Poly(allyl ether)-Based Cross-Linked Dual-Salt Polymer Electrolytes for High-Voltage Lithium Metal Batteries. ACS Applied Materials & Interfaces, 2020, 12, 567-579.	8.0	31
27	Scalable Synthesis of Manganese-Doped Hydrated Vanadium Oxide as a Cathode Material for Aqueous Zinc-Metal Battery. ACS Applied Materials & Interfaces, 2020, 12, 48542-48552.	8.0	21
28	An In Situ Cross‣inked Nonaqueous Polymer Electrolyte for Zincâ€Metal Polymer Batteries and Hybrid Supercapacitors. Small, 2020, 16, e2002528.	10.0	24
29	Hierarchical Nanoflower Arrays of Co ₉ S ₈ â€Ni ₃ S ₂ on Nickel Foam: A Highly Efficient Binderâ€Free Electrocatalyst for Overall Water Splitting. Chemistry - A European Journal, 2020, 26, 7900-7911.	3.3	22
30	Role of B site ions in bifunctional oxygen electrocatalysis: a structure–property correlation study on doped Ca ₂ Fe ₂ O ₅ brownmillerites. Physical Chemistry Chemical Physics, 2020, 22, 15520-15527.	2.8	3
31	A NiFe layered double hydroxide-decorated N-doped entangled-graphene framework: a robust water oxidation electrocatalyst. Nanoscale Advances, 2020, 2, 1709-1717.	4.6	21
32	Template assisted synthesis of Ni,N co-doped porous carbon from Ni incorporated ZIF-8 frameworks for electrocatalytic oxygen reduction reaction. New Journal of Chemistry, 2020, 44, 12343-12354.	2.8	15
33	Co 9 S 8 Nanoparticleâ€Supported Nitrogenâ€doped Carbon as a Robust Catalyst for Oxygen Reduction Reaction in Both Acidic and Alkaline Conditions. ChemElectroChem, 2020, 7, 3123-3134.	3.4	3
34	FeN _{<i>x</i>} /FeS _{<i>x</i>} -Anchored Carbon Sheet–Carbon Nanotube Composite Electrocatalysts for Oxygen Reduction. ACS Applied Nano Materials, 2020, 3, 2234-2245.	5.0	12
35	Nafion Ionomer-Based Single Component Electrolytes for Aqueous Zn/MnO ₂ Batteries with Long Cycle Life. ACS Sustainable Chemistry and Engineering, 2020, 8, 5040-5049.	6.7	37
36	Fe3+ stabilized 3D cross-linked glycine-melamine formaldehyde networks as precursor for highly efficient oxygen reduction catalyst in alkaline media. Materials Letters, 2020, 264, 127365.	2.6	4

#	Article	IF	CITATIONS
37	WO ₃ Nanorods Bearing Interconnected Pt Nanoparticle Units as an Activity-Modulated and Corrosion-Resistant Carbon-Free System for Polymer Electrolyte Membrane Fuel Cells. ACS Applied Energy Materials, 2020, 3, 1908-1921.	5.1	20
38	Co@CoAl‣ayered Double Hydroxide/Nitrogenâ€Doped Graphene Composite Catalyst for Alâ~H ₂ Oâ€Based Batteries: Simultaneous Hydrogen Production and Electricity Generation. ChemElectroChem, 2020, 7, 2582-2591.	3.4	11
39	Porphyrinâ€Based Conducting Polymer Hydrogel for Supercapacitor Application. Energy Technology, 2020, 8, 2000061.	3.8	16
40	Zinc-Ion Conducting Nonaqueous Polymer Electrolyte for Zinc-Metal Batteries through UV-Light Induced Cross-Linking Polymerization. ECS Meeting Abstracts, 2020, MA2020-02, 825-825.	0.0	0
41	Weak Intermolecular Interactions in Covalent Organic Framework-Carbon Nanofiber Based Crystalline yet Flexible Devices. ACS Applied Materials & Interfaces, 2019, 11, 30828-30837.	8.0	54
42	In-situ generated Mn3O4-reduced graphene oxide nanocomposite for oxygen reduction reaction and isolated reduced graphene oxide for supercapacitor applications. Carbon, 2019, 154, 285-291.	10.3	38
43	Carbon Derived from Soft Pyrolysis of a Covalent Organic Framework as a Support for Small-Sized RuO ₂ Showing Exceptionally Low Overpotential for Oxygen Evolution Reaction. ACS Omega, 2019, 4, 13465-13473.	3.5	33
44	Zinc ion interactions in a two-dimensional covalent organic framework based aqueous zinc ion battery. Chemical Science, 2019, 10, 8889-8894.	7.4	220
45	NiCo ₂ O ₄ nanoarray on CNT sponge: a bifunctional oxygen electrode material for rechargeable Zn–air batteries. Nanoscale Advances, 2019, 1, 3243-3251.	4.6	16
46	[MoS ₄] ^{2–} -Intercalated NiCo-Layered Double Hydroxide Nanospikes: An Efficiently Synergized Material for Urine To Direct H ₂ Generation. ACS Applied Materials & Interfaces, 2019, 11, 25917-25927.	8.0	23
47	Glycineâ€Induced Electrodeposition of Nanostructured Cobalt Hydroxide: A Bifunctional Catalyst for Overall Water Splitting. ChemSusChem, 2019, 12, 5300-5309.	6.8	6
48	Imidazole-Linked Crystalline Two-Dimensional Polymer with Ultrahigh Proton-Conductivity. Journal of the American Chemical Society, 2019, 141, 14950-14954.	13.7	148
49	Fe ₂ P ₄ O ₁₂ –carbon composite as a highly stable electrode material for electrochemical capacitors. New Journal of Chemistry, 2019, 43, 399-406.	2.8	16
50	Dendrite Growth Suppression by Zn ²⁺ â€Integrated Nafion Ionomer Membranes: Beyond Porous Separators toward Aqueous Zn/V ₂ O ₅ Batteries with Extended Cycle Life. Energy Technology, 2019, 7, 1900442.	3.8	76
51	A copper(<scp>ii</scp>)-coordination polymer based on a sulfonic–carboxylic ligand exhibits high water-facilitated proton conductivity. Dalton Transactions, 2019, 48, 11034-11044.	3.3	7
52	Cubic Palladium Nanorattles with Solid Octahedron Gold Core for Catalysis and Alkaline Membrane Fuel Cell Applications. ChemCatChem, 2019, 11, 4383-4392.	3.7	12
53	Coexisting Few-Layer Assemblies of NiO and MoO ₃ Deposited on Vulcan Carbon as an Efficient and Durable Electrocatalyst for Water Oxidation. ACS Applied Energy Materials, 2019, 2, 4987-4998.	5.1	15
54	Medium Modulated Oxygen Reduction Activity of Fe/Co Active Centreâ€engrafted Electrocatalysts. ChemElectroChem, 2019, 6, 2956-2964.	3.4	4

#	Article	IF	CITATIONS
55	A 3-D nanoribbon-like Pt-free oxygen reduction reaction electrocatalyst derived from waste leather for anion exchange membrane fuel cells and zinc-air batteries. Nanoscale, 2019, 11, 7893-7902.	5.6	34
56	High-Performing PGM-Free AEMFC Cathodes from Carbon-Supported Cobalt Ferrite Nanoparticles. Catalysts, 2019, 9, 264.	3.5	53
57	Graphene-modified electrodes for sensing doxorubicin hydrochloride in human plasma. Analytical and Bioanalytical Chemistry, 2019, 411, 1509-1516.	3.7	39
58	Rylene Diimide-Based Alternate and Random Copolymers for Flexible Supercapacitor Electrode Materials with Exceptional Stability and High Power Density. Journal of Physical Chemistry C, 2019, 123, 2084-2093.	3.1	30
59	Bifunctional Oxygen Reduction and Evolution Activity in Brownmillerites Ca ₂ Fe _(1–<i>x</i>) Co _{<i>x</i>} O ₅ . ACS Omega, 2019, 4, 31-38.	3.5	14
60	Synthesis of Ultrathin PEDOT on Carbon Nanotubes and Shear Thinning Xanthan Gumâ€H 2 SO 4 Gel Electrolyte for Supercapacitors. ChemElectroChem, 2019, 6, 1861-1869.	3.4	16
61	Studies on nano composites of SPEEK/ethylene glycol/cellulose nanocrystals as promising proton exchange membranes. Electrochimica Acta, 2019, 293, 260-272.	5.2	71
62	A rationally designed self-standing V ₂ O ₅ electrode for high voltage non-aqueous all-solid-state symmetric (2.0 V) and asymmetric (2.8 V) supercapacitors. Nanoscale, 2018, 10, 8741-8751.	5.6	30
63	Sensitive electrochemical detection of cardiac troponin I in serum and saliva by nitrogen-doped porous reduced graphene oxide electrode. Sensors and Actuators B: Chemical, 2018, 262, 180-187.	7.8	108
64	Porous reduced graphene oxide modified electrodes for the analysis of protein aggregation. Part 2: Application to the analysis of calcitonin containing pharmaceutical formulation. Electrochimica Acta, 2018, 266, 364-372.	5.2	5
65	Nucleic aptamer modified porous reduced graphene oxide/MoS2 based electrodes for viral detection: Application to human papillomavirus (HPV). Sensors and Actuators B: Chemical, 2018, 262, 991-1000.	7.8	82
66	Graphene with Fe and S Coordinated Active Centers: An Active Competitor for the Fe–N–C Active Center for Oxygen Reduction Reaction in Acidic and Basic pH Conditions. ACS Applied Energy Materials, 2018, 1, 368-376.	5.1	36
67	Water mediated proton conductance in a hydrogen-bonded Ni(<scp>ii</scp>)-bipyridine-glycoluril chloride self-assembled framework. CrystEngComm, 2018, 20, 1094-1100.	2.6	11
68	Naphthalene Diimide Copolymers by Direct Arylation Polycondensation as Highly Stable Supercapacitor Electrode Materials. Macromolecules, 2018, 51, 954-965.	4.8	47
69	Zirconium-Substituted Cobalt Ferrite Nanoparticle Supported N-doped Reduced Graphene Oxide as an Efficient Bifunctional Electrocatalyst for Rechargeable Zn–Air Battery. ACS Catalysis, 2018, 8, 3715-3726.	11.2	75
70	Iron Catalyzed Hydroformylation of Alkenes under Mild Conditions: Evidence of an Fe(II) Catalyzed Process. Journal of the American Chemical Society, 2018, 140, 4430-4439.	13.7	38
71	Realizing High Capacitance and Rate Capability in Polyaniline by Enhancing the Electrochemical Surface Area through Induction of Superhydrophilicity. ACS Applied Materials & Interfaces, 2018, 10, 676-686.	8.0	45
72	Melamine formaldehyde–metal organic gel interpenetrating polymer network derived intrinsic Fe–N-doped porous graphitic carbon electrocatalysts for oxygen reduction reaction. New Journal of Chemistry, 2018, 42, 18690-18701.	2.8	19

#	Article	IF	CITATIONS
73	Layered TiO ₂ Nanosheetâ€Supported NiCo ₂ O ₄ Nanoparticles as Bifunctional Electrocatalyst for Overall Water Splitting. ChemElectroChem, 2018, 5, 4000-4007.	3.4	18
74	Metalloporphyrin Two-Dimensional Polymers via Metal-Catalyst-Free C–C Bond Formation for Efficient Catalytic Hydrogen Evolution. ACS Applied Energy Materials, 2018, 1, 6442-6450.	5.1	27
75	Superprotonic Conductivity in Flexible Porous Covalent Organic Framework Membranes. Angewandte Chemie, 2018, 130, 11060-11064.	2.0	70
76	Superprotonic Conductivity in Flexible Porous Covalent Organic Framework Membranes. Angewandte Chemie - International Edition, 2018, 57, 10894-10898.	13.8	207
77	Preparation and investigations of ABPBI membrane for HT-PEMFC by immersion precipitation method. Journal of Membrane Science, 2018, 564, 211-217.	8.2	22
78	Convergent Covalent Organic Framework Thin Sheets as Flexible Supercapacitor Electrodes. ACS Applied Materials & Interfaces, 2018, 10, 28139-28146.	8.0	134
79	Repeated photoporation with graphene quantum dots enables homogeneous labeling of live cells with extrinsic markers for fluorescence microscopy. Light: Science and Applications, 2018, 7, 47.	16.6	50
80	Water-in-Acid Gel Polymer Electrolyte Realized through a Phosphoric Acid-Enriched Polyelectrolyte Matrix toward Solid-State Supercapacitors. ACS Sustainable Chemistry and Engineering, 2018, 6, 12630-12640.	6.7	17
81	Morphological Ensembles of Nâ€Doped Porous Carbon Derived from ZIFâ€8/Feâ€Graphene Nanocomposites: Processing and Electrocatalytic Studies. ChemistrySelect, 2018, 3, 8688-8697.	1.5	8
82	Synthesis of Carbon Nanosheets and Nitrogen-Doped Carbon Nanosheets from Perylene Derivatives for Supercapacitor Application. ACS Applied Nano Materials, 2018, 1, 4576-4586.	5.0	10
83	Interlayer Hydrogen-Bonded Covalent Organic Frameworks as High-Performance Supercapacitors. Journal of the American Chemical Society, 2018, 140, 10941-10945.	13.7	339
84	Grafoil–Scotch tape-derived highly conducting flexible substrate and its application as a supercapacitor electrode. Nanoscale, 2017, 9, 3593-3600.	5.6	13
85	On demand electrochemical release of drugs from porous reduced graphene oxide modified flexible electrodes. Journal of Materials Chemistry B, 2017, 5, 6557-6565.	5.8	13
86	Proton conduction in a hydrogen-bonded complex of copper(<scp>ii</scp>)-bipyridine glycoluril nitrate. Dalton Transactions, 2017, 46, 6968-6974.	3.3	15
87	Enhanced proton conduction by post-synthetic covalent modification in a porous covalent framework. Journal of Materials Chemistry A, 2017, 5, 13659-13664.	10.3	38
88	An all-solid-state-supercapacitor possessing a non-aqueous gel polymer electrolyte prepared using a UV-assisted in situ polymerization strategy. Journal of Materials Chemistry A, 2017, 5, 8461-8476.	10.3	83
89	Copper oxide supported on three-dimensional ammonia-doped porous reduced graphene oxide prepared through electrophoretic deposition for non-enzymatic glucose sensing. Electrochimica Acta, 2017, 224, 346-354.	5.2	53
90	Chitosan Intercalated Metal Organic Gel as a Green Precursor of Fe Entrenched and Fe Distributed N-Doped Mesoporous Graphitic Carbon for Oxygen Reduction Reaction. ChemistrySelect, 2017, 2, 8762-8770.	1.5	12

#	Article	IF	CITATIONS
91	Porous reduced graphene oxide modified electrodes for the analysis of protein aggregation. Part 1: Lysozyme aggregation at pH 2 and 7.4. Electrochimica Acta, 2017, 254, 375-383.	5.2	15
92	High-Level Supercapacitive Performance of Chemically Reduced Graphene Oxide. CheM, 2017, 3, 846-860.	11.7	68
93	Efficient and Durable Oxygen Reduction Electrocatalyst Based on CoMn Alloy Oxide Nanoparticles Supported Over N-Doped Porous Graphene. ACS Catalysis, 2017, 7, 6700-6710.	11.2	104
94	Activity Tuning of Cobalt Ferrite Nanoparticles Anchored on Nâ€Đoped Reduced Graphene Oxide as a Potential Oxygen Reduction Electrocatalyst by Zn Substitution in the Spinel Matrix. ChemistrySelect, 2017, 2, 7845-7853.	1.5	7
95	Selective isolation and eradication of E. coli associated with urinary tract infections using anti-fimbrial modified magnetic reduced graphene oxide nanoheaters. Journal of Materials Chemistry B, 2017, 5, 8133-8142.	5.8	23
96	Nitrogenâ€Doped Graphene with a Threeâ€Dimensional Architecture Assisted by Carbon Nitride Tetrapods as an Efficient Metalâ€Free Electrocatalyst for Hydrogen Evolution. ChemElectroChem, 2017, 4, 2643-2652.	3.4	29
97	NiZn double hydroxide nanosheet-anchored nitrogen-doped graphene enriched with the $\hat{1}^3$ -NiOOH phase as an activity modulated water oxidation electrocatalyst. Nanoscale, 2017, 9, 12590-12600.	5.6	64
98	Magnetic reduced graphene oxide loaded hydrogels: Highly versatile and efficient adsorbents for dyes and selective Cr(VI) ions removal. Journal of Colloid and Interface Science, 2017, 507, 360-369.	9.4	72
99	Ultrahigh Ionic Conduction in Water-Stable Close-Packed Metal-Carbonate Frameworks. Inorganic Chemistry, 2017, 56, 9710-9715.	4.0	1
100	Single Cell Fabrication Towards the Realistic Evaluation of a CNTâ€6trung ZIFâ€Derived Electrocatalyst as a Cathode Material in Alkaline Fuel Cells and Metalâ^'Air Batteries. ChemElectroChem, 2017, 4, 2928-2933.	3.4	23
101	Nitrogen-doped graphene anchored with mixed growth patterns of CuPt alloy nanoparticles as a highly efficient and durable electrocatalyst for the oxygen reduction reaction in an alkaline medium. Nanoscale, 2017, 9, 9009-9017.	5.6	25
102	N-doped porous reduced graphene oxide as an efficient electrode material for high performance flexible solid-state supercapacitor. Applied Materials Today, 2017, 8, 141-149.	4.3	69
103	Post-synthetically modified porous covalent framework (PCF) for high proton conduction. Acta Crystallographica Section A: Foundations and Advances, 2017, 73, C1156-C1156.	0.1	0
104	1D Alignment of PEDOT in a Buckypaper for Highâ€Performance Solid Supercapacitors. ChemElectroChem, 2016, 3, 1329-1336.	3.4	15
105	Multifunctional copper dimer: structure, band gap energy, catalysis, magnetism, oxygen reduction reaction and proton conductivity. RSC Advances, 2016, 6, 37515-37521.	3.6	11
106	Graphene Oxide Sheathed ZIF-8 Microcrystals: Engineered Precursors of Nitrogen-Doped Porous Carbon for Efficient Oxygen Reduction Reaction (ORR) Electrocatalysis. ACS Applied Materials & Interfaces, 2016, 8, 29373-29382.	8.0	139
107	Hydrogenâ€Bonded Organic Frameworks (HOFs): A New Class of Porous Crystalline Proton onducting Materials. Angewandte Chemie - International Edition, 2016, 55, 10667-10671.	13.8	334
108	Hydrogenâ€Bonded Organic Frameworks (HOFs): A New Class of Porous Crystalline Proton onducting Materials. Angewandte Chemie, 2016, 128, 10825-10829.	2.0	76

#	Article	IF	CITATIONS
109	Low Band Gap Benzimidazole COF Supported Ni ₃ N as Highly Active OER Catalyst. Advanced Energy Materials, 2016, 6, 1601189.	19.5	182
110	Strategic Preparation of Efficient and Durable NiCo Alloy Supported Nâ€Đoped Porous Graphene as an Oxygen Evolution Electrocatalyst: A Theoretical and Experimental Investigation. Advanced Materials Interfaces, 2016, 3, 1600532.	3.7	50
111	Valorization of coffee bean waste: a coffee bean waste derived multifunctional catalyst for photocatalytic hydrogen production and electrocatalytic oxygen reduction reactions. RSC Advances, 2016, 6, 82103-82111.	3.6	19
112	Cobalt Ferrite Bearing Nitrogen-Doped Reduced Graphene Oxide Layers Spatially Separated with Microporous Carbon as Efficient Oxygen Reduction Electrocatalyst. ACS Applied Materials & Interfaces, 2016, 8, 20730-20740.	8.0	41
113	Reduced Graphene Oxide Modified Electrodes for Sensitive Sensing of Gliadin in Food Samples. ACS Sensors, 2016, 1, 1462-1470.	7.8	57
114	1000-fold enhancement in proton conductivity of a MOF using post-synthetically anchored proton transporters. Scientific Reports, 2016, 6, 32489.	3.3	22
115	High-index faceted Au nanocrystals with highly controllable optical properties and electro-catalytic activity. Nanoscale, 2016, 8, 19224-19228.	5.6	13
116	Nanoporous Graphene Enriched with Fe/Coâ€N Active Sites as a Promising Oxygen Reduction Electrocatalyst for Anion Exchange Membrane Fuel Cells. Advanced Functional Materials, 2016, 26, 2150-2162.	14.9	305
117	Lowâ€Overpotential Electrocatalytic Water Splitting with Nobleâ€Metalâ€Free Nanoparticles Supported in a sp ³ Nâ€Rich Flexible COF. Advanced Energy Materials, 2016, 6, 1600110.	19.5	121
118	High hydroxide conductivity in a chemically stable crystalline metal–organic framework containing a water-hydroxide supramolecular chain. Chemical Communications, 2016, 52, 8459-8462.	4.1	32
119	Understanding the electron transfer process in ZnO–naphthol azobenzoic acid composites from photophysical characterisation. Physical Chemistry Chemical Physics, 2016, 18, 22179-22187.	2.8	3
120	Cobalt-Modified Covalent Organic Framework as a Robust Water Oxidation Electrocatalyst. Chemistry of Materials, 2016, 28, 4375-4379.	6.7	368
121	Unravelling the Mechanism of Electrochemical Degradation of PANI in Supercapacitors: Achieving a Feasible Solution. ChemElectroChem, 2016, 3, 933-942.	3.4	10
122	A mechanochemically synthesized covalent organic framework as a proton-conducting solid electrolyte. Journal of Materials Chemistry A, 2016, 4, 2682-2690.	10.3	309
123	Nitrogen and sulphur co-doped crumbled graphene for the oxygen reduction reaction with improved activity and stability in acidic medium. Journal of Materials Chemistry A, 2016, 4, 6014-6020.	10.3	46
124	Coordination polymers of Fe(<scp>iii</scp>) and Al(<scp>iii</scp>) ions with TCA ligand: distinctive fluorescence, CO ₂ uptake, redox-activity and oxygen evolution reaction. Dalton Transactions, 2016, 45, 6901-6908.	3.3	17
125	Pt- and TCO-Free Flexible Cathode for DSSC from Highly Conducting and Flexible PEDOT Paper Prepared via in Situ Interfacial Polymerization. ACS Applied Materials & Interfaces, 2016, 8, 553-562.	8.0	40
126	High-Performance Flexible Solid-State Supercapacitor with an Extended Nanoregime Interface through in Situ Polymer Electrolyte Generation. ACS Applied Materials & Interfaces, 2016, 8, 1233-1241.	8.0	59

#	Article	IF	CITATIONS
127	Pb ²⁺ —N Bonding Chemistry: Recycling of Polyaniline–Pb Nanocrystals Waste for Generating High-Performance Supercapacitor Electrodes. Journal of Physical Chemistry C, 2016, 120, 911-918.	3.1	16
128	Conjugated porous polymers as precursors for electrocatalysts and storage electrode materials. Chemical Communications, 2016, 52, 316-318.	4.1	40
129	<i>In vitro</i> and <i>in silico</i> antifungal efficacy of nitrogen-doped carbon nanohorn (NCNH) against <i>Rhizoctonia solani</i> . Journal of Biomolecular Structure and Dynamics, 2016, 34, 152-162.	3.5	20
130	CoSe ₂ Supported on Nitrogenâ€Doped Carbon Nanohorns as a Methanolâ€Tolerant Cathode for Airâ€Breathing Microlaminar Flow Fuel Cells. ChemElectroChem, 2015, 2, 1339-1345.	3.4	35
131	Lithiumâ€Assisted Proton Conduction at 150 °C in a Microporous Triazineâ€Phenol Polymer. Advanced Materials Interfaces, 2015, 2, 1500301.	3.7	11
132	Coherent Fusion of Water Array and Protonated Amine in a Metal–Sulfate-Based Coordination Polymer for Proton Conduction. Inorganic Chemistry, 2015, 54, 5366-5371.	4.0	16
133	Electrochemical preparation of nitrogen-doped graphene quantum dots and their size-dependent electrocatalytic activity for oxygen reduction. Bulletin of Materials Science, 2015, 38, 435-442.	1.7	32
134	Effect of B Site Coordination Environment in the ORR Activity in Disordered Brownmillerites Ba ₂ In _{2–<i>x</i>} Ce _{<i>x</i>} O _{5+δ} . ACS Applied Materials & Interfaces, 2015, 7, 3041-3049.	8.0	21
135	Novel scalable synthesis of highly conducting and robust PEDOT paper for a high performance flexible solid supercapacitor. Energy and Environmental Science, 2015, 8, 1339-1347.	30.8	350
136	Cu–Pt Nanocage with 3-D Electrocatalytic Surface as an Efficient Oxygen Reduction Electrocatalyst for a Primary Zn–Air Battery. ACS Catalysis, 2015, 5, 1445-1452.	11.2	103
137	Surface-modified single wall carbon nanohorn as an effective electrocatalyst for platinum-free fuel cell cathodes. Journal of Materials Chemistry A, 2015, 3, 4361-4367.	10.3	47
138	Switching Closed-Shell to Open-Shell Phenalenyl: Toward Designing Electroactive Materials. Journal of the American Chemical Society, 2015, 137, 5955-5960.	13.7	47
139	3D Polyaniline Porous Layer Anchored Pillared Graphene Sheets: Enhanced Interface Joined with High Conductivity for Better Charge Storage Applications. ACS Applied Materials & Interfaces, 2015, 7, 7661-7669.	8.0	68
140	Nanocrystalline Fe–Fe ₂ O ₃ particle-deposited N-doped graphene as an activity-modulated Pt-free electrocatalyst for oxygen reduction reaction. Nanoscale, 2015, 7, 20117-20125.	5.6	58
141	Can enantiomer ligands produce structurally distinct homochiral MOFs?. CrystEngComm, 2015, 17, 8202-8206.	2.6	18
142	Carbon Nanohorn-Derived Graphene Nanotubes as a Platinum-Free Fuel Cell Cathode. ACS Applied Materials & Interfaces, 2015, 7, 24256-24264.	8.0	67
143	Surface-Tuned Co ₃ O ₄ Nanoparticles Dispersed on Nitrogen-Doped Graphene as an Efficient Cathode Electrocatalyst for Mechanical Rechargeable Zinc–Air Battery Application. ACS Applied Materials & Interfaces, 2015, 7, 21138-21149.	8.0	145
144	Layer-separated MoS ₂ bearing reduced graphene oxide formed by an in situ intercalation-cum-anchoring route mediated by Co(OH) ₂ as a Pt-free electrocatalyst for oxygen reduction. Nanoscale, 2015, 7, 16729-16736.	5.6	36

#	Article	IF	CITATIONS
145	Low Surface Energy Plane Exposed Co ₃ O ₄ Nanocubes Supported on Nitrogen-Doped Graphene as an Electrocatalyst for Efficient Water Oxidation. ACS Applied Materials & Interfaces, 2015, 7, 442-451.	8.0	108
146	Fe(<scp>iii</scp>) phytate metallogel as a prototype anhydrous, intermediate temperature proton conductor. Chemical Science, 2015, 6, 603-607.	7.4	90
147	Nitrogen-Induced Surface Area and Conductivity Modulation of Carbon Nanohorn and Its Function as an Efficient Metal-Free Oxygen Reduction Electrocatalyst for Anion-Exchange Membrane Fuel Cells. Small, 2015, 11, 352-360.	10.0	83
148	A Covalent Organic Framework–Cadmium Sulfide Hybrid as a Prototype Photocatalyst for Visibleâ€Lightâ€Driven Hydrogen Production. Chemistry - A European Journal, 2014, 20, 15961-15965.	3.3	217
149	Electrodeposited polyethylenedioxythiophene with infiltrated gel electrolyte interface: a close contest of an all-solid-state supercapacitor with its liquid-state counterpart. Nanoscale, 2014, 6, 5944.	5.6	85
150	Twoâ€inâ€One: Inherent Anhydrous and Waterâ€Assisted High Proton Conduction in a 3D Metal–Organic Framework. Angewandte Chemie - International Edition, 2014, 53, 2638-2642.	13.8	367
151	Electrochemically grown nanoporous MnO2 nanowalls on a porous carbon substrate with enhanced capacitance through faster ionic and electrical mobility. Chemical Communications, 2014, 50, 7188.	4.1	34
152	Synthesis of an efficient heteroatom-doped carbon electro-catalyst for oxygen reduction reaction by pyrolysis of protein-rich pulse flour cooked with SiO2 nanoparticles. Physical Chemistry Chemical Physics, 2014, 16, 4251.	2.8	45
153	Structure and Dynamics of Benzyl-NX3 (X = Me, Et) Trifluoromethanesulfonate Ionic Liquids. Journal of Physical Chemistry B, 2014, 118, 1831-1838.	2.6	6
154	Layer-separated distribution of nitrogen doped graphene by wrapping on carbon nitride tetrapods for enhanced oxygen reduction reactions in acidic medium. Chemical Communications, 2014, 50, 13769-13772.	4.1	24
155	Activated nitrogen doped graphene shell towards electrochemical oxygen reduction reaction by its encapsulation on Au nanoparticle (Au@N-Gr) in water-in-oil "nanoreactors― Journal of Materials Chemistry A, 2014, 2, 1383-1390.	10.3	35
156	Post modification of MOF derived carbon via g-C ₃ N ₄ entrapment for an efficient metal-free oxygen reduction reaction. Chemical Communications, 2014, 50, 3363-3366.	4.1	145
157	Enhanced catalytic activity of polyethylenedioxythiophene towards tri-iodide reduction in DSSCs <i>via</i> 1-dimensional alignment using hollow carbon nanofibers. Nanoscale, 2014, 6, 10332-10339.	5.6	18
158	A Distinctive PdCl ₂ -Mediated Transformation of Fe-Based Metallogels into Metal–Organic Frameworks. Crystal Growth and Design, 2014, 14, 3434-3437.	3.0	35
159	Nanoporous graphene by quantum dots removal from graphene and its conversion to a potential oxygen reduction electrocatalyst via nitrogen doping. Energy and Environmental Science, 2014, 7, 1059.	30.8	156
160	From Waste Paper Basket to Solid State and Liâ€HEC Ultracapacitor Electrodes: A Value Added Journey for Shredded Office Paper. Small, 2014, 10, 4395-4402.	10.0	73
161	Nitrogen-doped graphene interpenetrated 3D Ni-nanocages: efficient and stable water-to-dioxygen electrocatalysts. Nanoscale, 2014, 6, 13179-13187.	5.6	33
162	Redoxâ€Mediated Synthesis of Functionalised Graphene: A Strategy towards 2D Multifunctional Electrocatalysts for Energy Conversion Applications. ChemPlusChem, 2013, 78, 1296-1303.	2.8	6

#	Article	IF	CITATIONS
163	Porous Carbons from Nonporous MOFs: Influence of Ligand Characteristics on Intrinsic Properties of End Carbon. Crystal Growth and Design, 2013, 13, 4195-4199.	3.0	138
164	1-Dimensional confinement of porous polyethylenedioxythiophene using carbon nanofibers as a solid template: an efficient charge storage material with improved capacitance retention and cycle stability. RSC Advances, 2013, 3, 11877.	3.6	25
165	Effect of the viscosity of poly(benzimidazole) on the performance of a multifunctional electrocatalyst with an ideal interfacial structure. Journal of Materials Chemistry A, 2013, 1, 4265.	10.3	4
166	Porousâ€Organicâ€Frameworkâ€Templated Nitrogenâ€Rich Porous Carbon as a More Proficient Electrocatalyst than Pt/C for the Electrochemical Reduction of Oxygen. Chemistry - A European Journal, 2013, 19, 974-980.	3.3	91
167	3-Dimensionally self-assembled single crystalline platinum nanostructures on few-layer graphene as an efficient oxygen reduction electrocatalyst. RSC Advances, 2013, 3, 6913.	3.6	11
168	Carbon nanofiber–RuO2–poly(benzimidazole) ternary hybrids for improved supercapacitor performance. RSC Advances, 2013, 3, 2428.	3.6	25
169	Hierarchically Nanoperforated Graphene as a High Performance Electrode Material for Ultracapacitors. Small, 2013, 9, 2801-2809.	10.0	33
170	Zeolitic Imidazolate Framework (ZIF)â€Derived, Hollowâ€Core, Nitrogenâ€Doped Carbon Nanostructures for Oxygenâ€Reduction Reactions in PEFCs. Chemistry - A European Journal, 2013, 19, 9335-9342.	3.3	147
171	Design of a High Performance Thin All-Solid-State Supercapacitor Mimicking the Active Interface of Its Liquid-State Counterpart. ACS Applied Materials & Interfaces, 2013, 5, 13397-13404.	8.0	53
172	A 3D Hexaporous Carbon Assembled from Single‣ayer Graphene as High Performance Supercapacitor. ChemSusChem, 2012, 5, 2159-2164.	6.8	72
173	Hydrous RuO ₂ –carbon nanofiber electrodes with high mass and electrode-specific capacitance for efficient energy storage. Nanoscale, 2012, 4, 890-896.	5.6	77
174	Polybenzimidazole mediated N-doping along the inner and outer surfaces of a carbon nanofiber and its oxygen reduction properties. Journal of Materials Chemistry, 2012, 22, 23668.	6.7	16
175	One-dimensional confinement of a nanosized metal organic framework in carbon nanofibers for improved gas adsorption. Chemical Communications, 2012, 48, 2009.	4.1	96
176	Tuning the Functionality of a Carbon Nanofiber–Pt–RuO ₂ System from Charge Storage to Electrocatalysis. Inorganic Chemistry, 2012, 51, 9766-9774.	4.0	22
177	Activity Modulated Low Platium Content Oxygen Reduction Electrocatalysts Prepared by Inducing Nano-Order Dislocations on Carbon Nanofiber through N ₂ -Doping. Journal of Physical Chemistry C, 2012, 116, 14754-14763.	3.1	22
178	Graphene enriched with pyrrolic coordination of the doped nitrogen as an efficient metal-free electrocatalyst for oxygen reduction. Journal of Materials Chemistry, 2012, 22, 23506.	6.7	159
179	An efficient oxygen reduction electrocatalyst from graphene by simultaneously generating pores and nitrogen doped active sites. Journal of Materials Chemistry, 2012, 22, 23799.	6.7	136
180	Disordered Brownmillerite Ba ₂ InCeO _{5+δ} with Enhanced Oxygen Reduction Activity. Chemistry of Materials, 2012, 24, 2823-2828.	6.7	25

#	Article	IF	CITATIONS
181	Tuning the Performance of Low-Pt Polymer Electrolyte Membrane Fuel Cell Electrodes Derived from Fe ₂ O ₃ @Pt/C Core–Shell Catalyst Prepared by an in Situ Anchoring Strategy. Journal of Physical Chemistry C, 2012, 116, 7318-7326.	3.1	33
182	Trigol based reduction of graphite oxide to graphene with enhanced charge storage activity. Journal of Materials Chemistry, 2012, 22, 11140.	6.7	33
183	Highly exposed and activity modulated sandwich type Pt thin layer catalyst with enhanced utilization. Journal of Materials Chemistry, 2011, 21, 19039.	6.7	8
184	Facile construction of non-precious iron nitride-doped carbon nanofibers as cathode electrocatalysts for proton exchange membrane fuel cells. Chemical Communications, 2011, 47, 2910.	4.1	45
185	Improved performance of phosphonated carbon nanotube–polybenzimidazole composite membranes in proton exchange membrane fuel cells. Journal of Materials Chemistry, 2011, 21, 7223.	6.7	77
186	Enhanced electrocatalytic performance of functionalized carbon nanotube electrodes for oxygen reduction in proton exchange membrane fuel cells. Physical Chemistry Chemical Physics, 2011, 13, 10312.	2.8	31
187	Ex-situ dispersion of core–shell nanoparticles of Cu–Pt on an in situ modified carbon surface and their enhanced electrocatalytic activities. Chemical Communications, 2011, 47, 3951.	4.1	25
188	Application of Functionalized CNT–Polymer Composite Electrolytes for Enhanced Charge Storage in "All Solid-State Supercapacitors". Journal of Nano Energy and Power Research, 2011, 1, 42-48.	0.2	0
189	Pt–MoOx-carbon nanotube redox couple based electrocatalyst as a potential partner with polybenzimidazole membrane for high temperature Polymer Electrolyte Membrane Fuel Cell applications. Electrochimica Acta, 2010, 55, 2878-2887.	5.2	42
190	High Pt Utilization Electrodes for Polymer Electrolyte Membrane Fuel Cells by Dispersing Pt Particles Formed by a Preprecipitation Method on Carbon "Polished―with Polypyrrole. Journal of Physical Chemistry C, 2010, 114, 14654-14661.	3.1	58
191	Artificially Designed Membranes Using Phosphonated Multiwall Carbon Nanotubeâ~'Polybenzimidazole Composites for Polymer Electrolyte Fuel Cells. Journal of Physical Chemistry Letters, 2010, 1, 2109-2113.	4.6	64
192	Bio-inspired catalyst compositions for enhanced oxygen reduction using nanostructured Pt electrocatalysts in polymer electrolyte fuel cells. Journal of Materials Chemistry, 2010, 20, 9651.	6.7	5
193	High aspect ratio nanoscale multifunctional materials derived from hollow carbon nanofiber by polymer insertion and metal decoration. Chemical Communications, 2010, 46, 5590.	4.1	16
194	Design of an "all solid-state―supercapacitor based on phosphoric acid doped polybenzimidazole (PBI) electrolyte. Journal of Applied Electrochemistry, 2009, 39, 1097-1103.	2.9	45
195	Domain Size Manipulation of Perflouorinated Polymer Electrolytes by Sulfonic Acid-Functionalized MWCNTs To Enhance Fuel Cell Performance. Langmuir, 2009, 25, 8299-8305.	3.5	87
196	Carbon Nanofiber with Selectively Decorated Pt Both on Inner and Outer Walls as an Efficient Electrocatalyst for Fuel Cell Applications. Journal of Physical Chemistry C, 2009, 113, 17572-17578.	3.1	45
197	Stability Improvement of Rh/γ-Al2O3Catalyst Layer by Ceria Doping for Steam Reforming in an Integrated Catalytic Membrane Reactor System. Catalysis Letters, 2004, 92, 181-187.	2.6	36

198 Title is missing!. Catalysis Letters, 2003, 86, 273-278.

#	Article	IF	CITATIONS
199	Ferrospinels based on Co and Ni prepared via a low temperature route as efficient catalysts for the selective synthesis of o-cresol and 2,6-xylenol from phenol and methanol. Journal of Molecular Catalysis A, 2002, 185, 259-268.	4.8	79
200	A comparison on the catalytic activity of Zn1â^'xCoxFe2O4 (x = 0, 0.2, 0.5, 0.8 and 1.0)-type ferrospinels prepared via. a low temperature route for the alkylation of aniline and phenol using methanol as the alkylating agent. Applied Catalysis A: General, 2002, 230, 245-251.	4.3	42
201	Cu–Co Synergism in Cu1â^'xCoxFe2O4—Catalysis and XPS Aspects. Journal of Catalysis, 2002, 210, 405-417.	6.2	164
202	Vapor-phase methylation of pyridine with methanol to 3-picoline over Zn1â^'xCoxFe2O4 (x=0, 0.2, 0.5, 0.8) Tj ETQ 205, 11-18.	<u>0</u> q0 0 0 rgl 4.3	BT /Overlocl 35
203	Studies on gasoline fuel processor system for fuel-cell powered vehicles application. Applied Catalysis A: General, 2001, 215, 1-9.	4.3	76
204	Catalytic Activity of Rare Earth-Promoted SO42-/SnO2in the Oxidative Dehydrogenation of Ethylbenzene. Bulletin of the Chemical Society of Japan, 2000, 73, 1285-1290.	3.2	7
205	Chemoselective Transfer Hydrogenation Reactions over Calcined-Layered Double Hydroxides. Bulletin of the Chemical Society of Japan, 2000, 73, 1425-1427.	3.2	12
206	Selective N-monomethylation of aniline using Zn1â^'Co Fe2O4 (x=0, 0.2, 0.5, 0.8 and 1.0) type systems. Journal of Molecular Catalysis A, 2000, 152, 225-236.	4.8	13
207	Influence of acid–base properties of mixed oxides derived from hydrotalcite-like precursors in the transfer hydrogenation of propiophenone. Journal of Molecular Catalysis A, 2000, 157, 193-198.	4.8	48
208	Selective N-methylation of aniline with dimethyl carbonate over Zn1â^'xCoxFe2O4 (x=0, 0.2, 0.5, 0.8 and) Tj ETQq	0.0.0 rgB 4.8	Г /Qverlock
209	A comparative study on aniline alkylation activity using methanol and dimethyl carbonate as the alkylating agents over Zn–Co–Fe ternary spinel systems. Applied Catalysis A: General, 2000, 201, L1-L8.	4.3	27
210	Alkylation of Phenol with Methanol Over Rare Earth Promoted Sulfated Tin Oxide Catalyst. Reaction Kinetics and Catalysis Letters, 2000, 69, 339-343.	0.6	10
211	Title is missing!. Reaction Kinetics and Catalysis Letters, 2000, 70, 161-167.	0.6	2
212	Title is missing!. Catalysis Letters, 2000, 65, 99-105.	2.6	21
213	Selective Methylation of Phenol, Aniline and Catechol with Dimethyl Carbonate Over Calcined Mg-Al Hydrotalcites. Synthetic Communications, 2000, 30, 3929-3934.	2.1	15
214	NiO-Al2O3 Prepared From A Ni-Al Hydrotalcite Precursor As An Efficient Catalyst For Transfer Hydrogenation Reactions. Synthetic Communications, 2000, 30, 1573-1579.	2.1	19
215	Selective N-monomethylation of aniline over Zn1â^'xNixFe2O4 (x=0, 0.2, 0.5, 0.8 and 1) type systems. Applied Catalysis A: General, 1999, 182, 327-336.	4.3	25
216	Electron donor properties and catalytic activity of manganese ferrospinels. Reaction Kinetics and Catalysis Letters, 1999, 66, 39-45.	0.6	2

#	Article	IF	CITATIONS
217	Reduction of Aromatic Nitro Compounds with Hydrazine Hydrate over a CeO2–SnO2 Catalyst. Journal of Chemical Research Synopses, 1999, , 674-675.	0.3	15
218	Calcined Layered Double Hydroxides as Basic Heterogeneous Catalysts for the Oppenauer Oxidation of Alcohols. Bulletin of the Chemical Society of Japan, 1999, 72, 2117-2119.	3.2	14
219	Alkaline Water Electrolysis by NiZn-Double Hydroxide-Derived Porous Nickel Selenide-Nitrogen-Doped Graphene Composite. ACS Applied Energy Materials, 0, , .	5.1	8